Journal of Zhejiang University-SCIENCE C (Computers & Electronics)
ISSN 1869-1951 (Print); ISSN 1869-196X (Online)
www.zju.edu.cn/jzus; www.springerlink.com
E-mail: jzus@zju.edu.cn

Harmonic suppressed bandpass filter using composite right/left handed transmission line*

Jian-gang LIANG, He-xiu XU†‡

(*Electromagnetic Field and Microwave Technique, Missile Institute, Air Force Engineering University, Shaanxi 713800, China*)

†E-mail: hxxu20008@yahoo.cn

Received Dec. 30, 2011; Revision accepted Mar. 23, 2012; Crosschecked May 25, 2012

Abstract: A wideband composite right/left handed transmission line (CRLH TL) in conjunction with its corresponding equivalent circuit model is studied based on a cascaded complementary single split ring resonator (CCSSRR). The characterization is performed by theory analysis, circuit simulation, and full-wave electromagnetic (EM) simulation. The negative refractive index (NRI) and backward wave propagation performance of the CRLH TL are demonstrated. For application, a bandpass filter (BPF) with enhanced out-of-band selectivity and harmonic suppression operating at the wireless local area network (WLAN) band is designed, fabricated, and measured by combining the CRLH TL with a complementary electric inductive-capacitive resonator (CELC). Three CELC cells with wideband stopband performance in the conductor strip and ground plane, respectively, are utilized in terms of single negative permeability. The design concept has been verified by the measurement data.

Key words: Composite right/left handed transmission line, Cascaded complementary split single ring resonator, Bandpass filter, Complementary electric inductive-capacitive resonator (CELC), Negative permeability

doi:10.1631/jzus.C1100386 **Document code:** A **CLC number:** O441

1 Introduction

Since the complementary split ring resonators (CSRRs) were initially proposed by Falcone *et al*. (2004), the resonant-type composite right/left handed transmission line (CRLH TL) has emerged and attracted extensive attention in the field of metamaterials (MTMs). To date, it has led to a completely new concept and brought extensive applications in microwave filters, couplers, and antennas (García-García *et al*., 2005; Bonache *et al*., 2006; Niu, 2010; Xu *et al*., 2011c). Although these filters feature compactness, improved selectivity, and even harmonic suppression out of band, the left handed (LH) band is essentially narrow and deserves further research and improvement. The electric inductive-capacitive resonator (ELC) (Schurig *et al*., 2006) and its complementary counterpart (CELC) (Hand *et al*., 2008) have been demonstrated as an electric resonator and a magnetic resonator, respectively, in bulk MTMs. Concerning the microstrip CELC in the ground plane (Lu *et al*., 2008), single negative permeability is expected according to the Babinet principle and in turn the resultant signal inhibition characteristic can be adopted for harmonic suppression.

As to the previous low-pass filters with ultra wideband stopband characteristic (Mandal *et al*., 2006; Xu *et al*., 2011b), a chain of cells with different dimensions are preferably selected. Each cell provides a transmission zero contributing to out-of-band suppression over a specified frequency range. Although the design concept is straightforward and simple, the collection of multiple cells may increase the area of microwave circuits, which certainly conflicts with the recent trend of highly integrated circuit. Concerning the harmonic suppression of the bandpass filter (BPF), the aforementioned concept can be certainly utilized for this issue. A survey of literature

‡ Corresponding author

* Project (Nos. 60871027 and 60971118) supported by the National Natural Science Foundation of China

indicates that other technologies were also available, e.g., coupled BPF using fractal geometry (Kim *et al*., 2005; Chen and Wang, 2009), BPF with far out-of-band suppression below or above the passband by introducing transmission zeros (Tsai *et al*., 2003; Amari and Rosenberg, 2004). Although these BPFs have comparable out-of-band suppression, the synthesis of those transmission zeros is somewhat complicated, making the alternative, improved, and simplified design a pressing task.

In this paper, we perform a complementary study on the wideband CRLH TL based on a cascaded complementary single split ring resonator (CCSSRR) recently proposed by Xu *et al*. (2011a), followed by a novel BPF design through combining the CRLH TL with CELC. The BPF advances in terms of high performances including deep rejection in the harmonic, low in-band insertion loss, and steep rejection skirt in the transition band. The sub-wavelength dimensions and particular behavior are the main merits of CCSSRR and CELC.

2 Layout, equivalent circuit model, and analysis of CRLH TL

Fig. 1 plots the topology of the CRLH TL incorporating different cells in the propagation direction and the corresponding equivalent T-circuit model (irrespective of losses for easy analysis). As can be seen, a novel CRLH TL consists of a square CCSSRR (in white) etched in the ground plane (in light grey) and a series capacitive gap above the CCSSRR on the signal strip (in dark grey) for proper electric excitation. The CCSSRR is formed from a fundamental complementary single split ring resonator (CSSRR) with a center pole dividing the particle into two identical smaller CSSRRs and two splits symmetrically located in the center top side of each smaller CSSRR. Each CRLH cell is spaced by a w=4 mm access line. Notice that the conventional CRLH TL using a CSSRR can be referred to Xu *et al*. (2011b) and thus it is not reproduced here for brevity. For characterization, the CRLH TL with physical parameters g_1=g_2=0.2 mm, g_3=0.3 mm, w_3=6 mm is designed on the F4B-2 (North Electronic Engineering Research Institute, Xi'an, China) substrate with a thickness of 0.8 mm and a dielectric constant of 2.65.

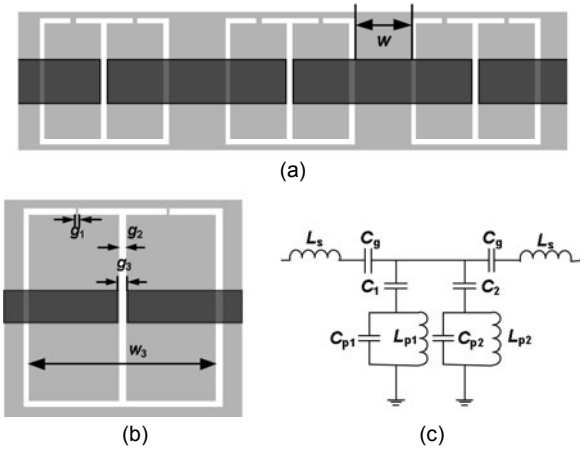

Fig. 1 Topology and the corresponding equivalent T-circuit model of the CRLH TL

(a) Three cells in the propagation direction; (b) Dimensional illustration of one cell; (c) Circuit model

Since the electric response of a novel CCSSRR is composed of two parts, namely, the primary excitation induced by the fundamental CSSRR with two splits and the second excitation by two identical smaller CSSRRs formed by the center pole and single split, two shunt branches should be adopted in the circuit model to represent these resultant effects (Xu *et al*., 2011a). In Fig. 1c, L_s models the line inductance, C_g models the gap capacitance, and C_1 represents the coupling effect between the conductor strip and the fundamental CSSRR which is described by means of a parallel resonant tank (L_{p1} and C_{p1}). Similarly, C_2 models the electric coupling between the line and small CSSRR which is characterized by means of a resonant tank (L_{p2} and C_{p2}). The two shunt branches in the circuit model distinguish the CRLH TL from any previous counterparts using CSSRR and CSRRs whose circuit models feature only one shunt branch.

Here, we begin with the research from circuit theory analysis. Given a CRLH TL with an N-cell ladder network, the transmission characteristic can be conveniently calculated using the [$ABCD$] matrix method (Caloz and Itoh, 2006). For one-cell CRLH TL, the [$ABCD$] matrix for the two-port network associated with the input and output voltage and current is formulated as follows:

$$\begin{bmatrix} V_{\text{in}} \\ I_{\text{in}} \end{bmatrix} = \begin{bmatrix} A & B \\ C & D \end{bmatrix} \begin{bmatrix} V_{\text{out}} \\ I_{\text{out}} \end{bmatrix}. \tag{1}$$

Note that the *ABCD* parameters can be easily transferred to scattering (*S*) parameters. Therefore, the transmission characteristic of the *N*-cell CRLH TL can be immediately obtained by cascading *N* two-port networks:

$$\begin{bmatrix} V_{\text{in}} \\ I_{\text{in}} \end{bmatrix} = \begin{bmatrix} A_N & B_N \\ C_N & D_N \end{bmatrix} \begin{bmatrix} V_{\text{out}} \\ I_{\text{out}} \end{bmatrix}, \tag{2}$$

where

$$\begin{bmatrix} A_N & B_N \\ C_N & D_N \end{bmatrix} = \prod_{k=1}^{N} \begin{bmatrix} A & B \\ C & D \end{bmatrix}^k. \tag{3}$$

Although the CRLH cells are identical (isotropic) and periodically cascaded in the current particular case for computation and fabrication convenience, it is not necessary to require this periodic and isotropic configuration. The [*ABCD*] matrix of the one-cell two-port network is related with the series impedance *Z* and total shunt admittance *Y* (two shunt branches) as follows:

$$\begin{aligned} \begin{bmatrix} A & B \\ C & D \end{bmatrix} &= \begin{bmatrix} 1 & Z/2 \\ 0 & 1 \end{bmatrix} \begin{bmatrix} 1 & 0 \\ Y & 1 \end{bmatrix} \begin{bmatrix} 1 & Z/2 \\ 0 & 1 \end{bmatrix} \\ &= \begin{bmatrix} 1+ZY/2 & Z(1+ZY/4) \\ Y & 1+ZY/2 \end{bmatrix}, \end{aligned} \tag{4}$$

where *Z* is associated with circuit elements, and

$$Z = \frac{2(1-\omega^2 L_{\text{s}} C_{\text{g}})}{\text{j}\omega C_{\text{g}}}. \tag{5}$$

The calculation of *Y* is somewhat sophisticated and can be attained as

$$\begin{aligned} Y = Y_1 + Y_2 &= \frac{\text{j}\omega(1-\omega^2 L_{\text{p1}} C_{\text{p1}})C_1}{1-\omega^2 L_{\text{p1}} C_{\text{p1}} - \omega^2 L_{\text{p1}} C_1} \\ &+ \frac{\text{j}\omega(1-\omega^2 L_{\text{p2}} C_{\text{p2}})C_2}{1-\omega^2 L_{\text{p2}} C_{\text{p2}} - \omega^2 L_{\text{p2}} C_2}. \end{aligned} \tag{6}$$

From Eq. (3), we conclude that the transmission characteristic of the *N*-cell CRLH TL is determined solely by that of the fundamental CRLH cell. Due to the two shunt branches in the circuit model, two transmission zeros are expected to be (Xu *et al*., 2011a)

$$\omega_{\text{z1}} = 2\pi f_{\text{z1}} = \frac{1}{\sqrt{L_{\text{p1}}(C_1 + C_{\text{p1}})}}, \tag{7}$$

$$\omega_{\text{z2}} = 2\pi f_{\text{z2}} = \frac{1}{\sqrt{L_{\text{p2}}(C_2 + C_{\text{p2}})}}. \tag{8}$$

Fig. 2 depicts the schematic of the CRLH TL constructed by periodically cascading a collection of unit-cell ladder networks. Since the CRLH TL is infinite and periodic, the input impedance Z_{in} should be the same at an arbitrary node. Therefore, we directly obtain the following equation:

$$\begin{aligned} Z_{\text{in}} &= Z + \left(\frac{1}{Y_1 + Y_2} \| Z_{\text{in}} \right) = Z + \frac{Z_{\text{in}}/(Y_1+Y_2)}{1/(Y_1+Y_2) + Z_{\text{in}}} \\ &= \frac{Z}{2}\left(1 \pm \sqrt{1 + \frac{4}{Z(Y_1+Y_2)}} \right). \end{aligned} \tag{9}$$

The real part of Z_{in}, $\text{Re}(Z_{\text{in}})$, takes poles when $Z(Y_1+Y_2)=0$, and takes zero when $Z(Y_1+Y_2)=-4$. In the lossless case, *Z* is purely imaginary. Consequently, the above two cases represent the changes in sign of $\text{Re}(Z_{\text{in}})$, and in turn correspond to the cutoff frequencies (Caloz and Itoh, 2006). The upper limit of the LH band (ω_{p}) and the lower limit of the right handed (RH) band (ω_{se}) are achieved by forcing *Y* and *Z* to be null (namely, the requirement in the first case), which yields

$$\begin{aligned} &(C_1 - \omega^2 L_{\text{p1}} C_{\text{p1}} C_1)(1 - \omega^2 L_{\text{p2}} C_{\text{p2}} - \omega^2 L_{\text{p2}} C_2) \\ &+ (C_2 - \omega^2 L_{\text{p2}} C_{\text{p2}} C_2)(1 - \omega^2 L_{\text{p1}} C_{\text{p1}} - \omega^2 L_{\text{p1}} C_1) = 0, \end{aligned} \tag{10}$$

$$1 - \omega^2 L_{\text{s}} C_{\text{g}} = 0. \tag{11}$$

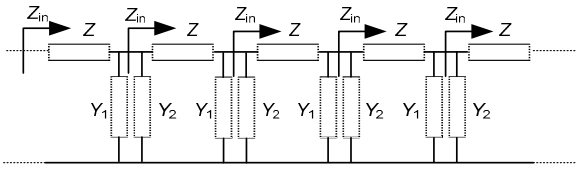

Fig. 2 Input impedance of CRLH TL with an infinite periodic ladder network

The CRLH TL is rigorously balanced only when $\omega_{\text{p}}=\omega_{\text{se}}$. The lower limit of the LH band ($\omega_{\text{LH}}^{\text{L}}$) and the upper limit of the RH band ($\omega_{\text{RH}}^{\text{H}}$), namely two cutoff frequencies, can be obtained by solving the

equation in the second case. The solving process is sophisticated and tedious; therefore, the analytic expressions of cutoff frequencies are not provided. However, they can be ambiguously identified from the transmission characteristic of a CRLH TL with a large number of cells. Note that the $\omega_{\mathrm{LH}}^{\mathrm{L}}$ and $\omega_{\mathrm{RH}}^{\mathrm{H}}$ of CRLH TL are not the transmission zeros (attenuation poles) that the two shunt branches provide. In general form, they fulfill the requirement of $\omega_{z1} \leq \omega_{\mathrm{LH}}^{\mathrm{L}} < \omega_{\mathrm{p}} \leq \omega_{\mathrm{se}} < \omega_{\mathrm{RH}}^{\mathrm{H}} \leq \omega_{z2}$.

For characterization, CRLH TLs depicted in Fig. 1 are investigated by means of moment-of-method (MOM) based planar electromagnetic (EM) simulation through Ansoft Designer together with electrical simulation through circuit simulated engine Ansoft Serenade. During the lumped parameters extraction process (electrical simulation), *S*-parameters of the circuit model are driven to match the EM simulated ones. Fig. 3 illustrates the EM simulated full-wave and electrically simulated *S*-parameters of the CRLH TL which has different cells in the propagation direction. It is unambiguous that these results are in desirable agreement in both cases, which has verified not only the rationality of the presented circuit model but also the extracted circuit elements.

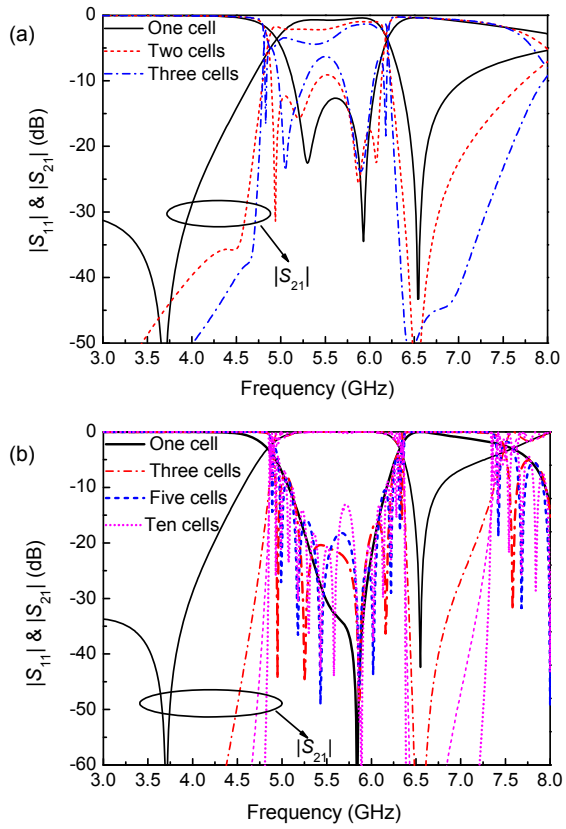

Fig. 3 *S*-parameters of CRLH TLs which have different cells in the propagation direction obtained from EM full-wave simulation (a) and circuit simulation (b)

After a further inspection, three most important aspects should be highlighted. Firstly, the novel CRLH TL obviously exhibits two transmission zeros around 3.7 and 6.5 GHz in the lower and upper edges of the transmission band, respectively. Secondly, the −10 dB impedance bandwidth of the CRLH TL ranging from 5.1 to 6.1 GHz has been significantly broadened with respect to 0.2 GHz of the conventional CSSRR-loaded CRLH TL with the same physical parameters. Thirdly, the lower and upper band skirt suppression and selectivity are enhanced significantly with the increase of the number of cells in both cases. Very accurate cutoff frequencies can be absolutely identified, especially when N=3 in the former case and N=10 in the latter case. The cutoff frequencies $f_{\mathrm{LH}}^{\mathrm{L}}$ =4.77 GHz and $f_{\mathrm{RH}}^{\mathrm{H}}$ =6.26 GHz in the former case are quantitatively very similar to $f_{\mathrm{LH}}^{\mathrm{L}}$ =4.83 GHz and $f_{\mathrm{RH}}^{\mathrm{H}}$ =6.38 GHz in the latter case.

The extracted circuit elements are listed as L_{s}=3.86 nH, C_{g}=0.20 pF, C_1=1.96 pF, C_2=0.82 pF, C_{p1}=0.20 pF, L_{p1}=0.85 nH, C_{p2}=7.66 pF, L_{p2}=0.07 nH. By inserting these lumped elements into Eqs. (7) and (8), two attenuation poles are obtained as 3.70 and 6.53 GHz, which are qualitatively very similar to those obtained from EM simulation. Consequently, we conclude that C_1, C_{p1}, and L_{p1} are responsible for the lower transmission zero while C_2, C_{p2}, and L_{p2} for the upper transmission zero. Note that the fundamental CSSRR for lower transmission zero is not intuitive and we have verified it from individual analysis of the fundamental CSSRR (i.e., by excluding the center pole from CCSSRR). As expected, the lower transmission zero obtained from this structure is 3.55 GHz, which is almost identical to that of CCSSRR. Note that perfect coincidence is impossible due to the effects of the center pole.

Since the negative permittivity of CSSRR and resultant LH characteristic of the CRLH TL have been successfully validated by the effective material parameters, they are not reproduced for brevity. Here, of particular interest is that we concentrate on the composite balanced LH and RH band characteristic. In this regard, Fig. 4 depicts the curve of refractive

index n and propagation constant β of one-cell CRLH TL from simulated S-parameters by using the improved retrieval method (Xu *et al*., 2011b). A very obvious negative refractive index and backward wave propagation can be obtained. It also indicates that the essential LH band which allows signal to transmit freely is in the scope of 4.90–5.65 GHz. In this range, the imaginary part of the refractive index, which accounts for electric and magnetic loss, is approximately zero. Above 5.65 GHz, a narrow RH band continues. Therefore, an exciting characteristic is that the balanced passband consists of not only an LH contribution but also an RH one.

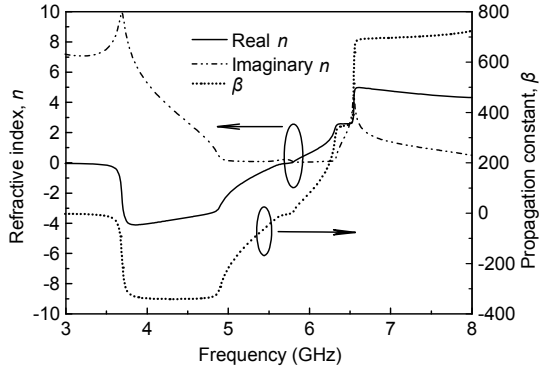

Fig. 4 Refractive index and propagation constant of the one-cell CRLH TL

3 Bandpass filter application

Based on the established circuit model and analysis of novel CRLH TL, it is easy for us to utilize the unique behavior of two transmission zeros to engineer a BPF. Note that the operating frequencies of CRLH TL (composite LH and RH bands) can be adjusted up and down to any arbitrarily specified band by scaling the dimensions of the CRLH cell. Despite this, the upper stopband bandwidth of the novel CRLH TL is still narrow and too insufficient for harmonic suppression above the passband. A multi-cell CRLH TL is able to enhance the lower and upper skirt selectivities; however, a collection of these cells may facilitate a large circuit area. In this regard, we consider using several CELC cells and locating their wide stopband above the edge of the RH band of the CRLH TL to address these problems.

It has been well established that the rejection level and stopband bandwidth increase with the number of particles adopted (Mandal *et al*., 2006; Xu *et al*., 2011b). In the current design, three CELC cells and one CRLH cell are considered. Double-layer CELC pattern is utilized to facilitate the integrated circuit, which is a tradeoff between miniaturization and good upper band skirt performance. The two alternative types of CELC allow additional flexibility in BPF design. Topology of the eventually designed BPF is shown in Fig. 5. It has been well established that the stopband of CELC in the ground emerges, attributing to single negative permeability in the vicinity of magnetic resonance (Lu *et al*., 2008). The transmission zero can be controlled by a distance length L and a pole height h.

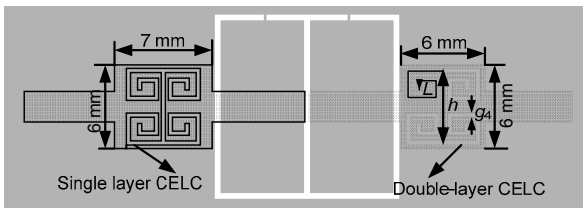

Fig. 5 Topology of the proposed BPF using a CCSSRR-loaded CRLH cell and CELC

The CRLH cell is embedded in the center, whereas three CELC cells are located in both ends with two of them in the conductor strip and the leftover one (below) in the ground plane. The structure parameters of three CELC cells are kept identical

Here, we concentrate on the study of a novel CELC in the conductor strip for comprehensive understanding of the performances and mechanisms. For characterization, the F4B-2 substrate with a thickness of 0.8 mm and a dielectric constant of 2.65 is applied for design including the forthcoming BPF. The optimized physical parameters of three CELC cells are L=14.4 mm, h=5.5 mm, and g_4=0.3 mm. Fig. 6 shows the simulated full-wave S-parameters and retrieved constitutive EM parameters obtained from n and effective impedance z (Xu *et al*., 2011b). According to Fig. 6a, a very wide stopband with two additional transmission zeros is achieved. By referring to Fig. 6b, we conclude that magnetic resonance is responsible for the first transmission zero while electric resonance for the second one. The wide stopband is engineered due to the merging of the two resonances. If h were selected to be a little larger, a passband would have emerged between them.

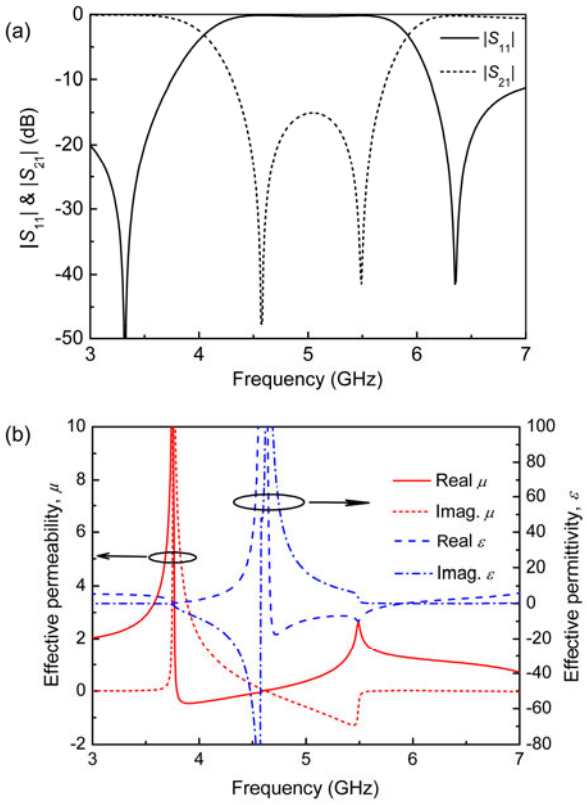

Fig. 6 Results of the proposed CELC in the conductor strip
(a) *S*-parameters; (b) Effective permeability and permittivity

To provide controllability over these attenuation poles and guidelines for generic design, we have performed extensive simulations providing structure parameter analysis. For brevity these results are not provided. Here we review our efforts and draw directly the useful conclusion. The value of g_4 has little influence on these two transmission zeros. The increased L shifts both transmission zeros downwards, and narrows the stopband bandwidth because the upper transmission zero shrinks even faster than the lower fundamental one. The increase of h makes both transmission zeros shift upward. However, the strength effect of the lower transmission zero is much weaker than that of the upper one, and thus the stopband bandwidth is enhanced.

For verification, the proposed BPF operating at 2.45 GHz has been fabricated and measured (through an Anritsu ME7808A vector network analyzer). Fig. 7 insets the fabricated prototype of the engineered BPF. It is compact with an occupied area of 39.4 mm×22 mm. Detailed dimensions of CCSSRR are optimized as g_1=g_2=g_3=0.3 mm, w_3=12.8 mm. Fig. 7 also shows the simulated and measured *S*-parameters of the fabricated BPF. Very reasonable agreement is observed in the whole frequency band of interest. The measured −10 dB impedance bandwidth ranges from 2.28 to 2.70 GHz, in which the insertion loss is lower than 1.2 dB. Two transmission zeros located in the lower and upper edge bands have increased the practical selectivity to up to 38.6 and 56.6 dB/GHz, respectively. In the upper out-of-band skirt, the signal inhibition is lower than 35 dB at the first harmonic 4.9 GHz, while the total suppression is lower than 14 dB. Therefore, the engineered filter advances in harmonic suppression, compact footprint, and a great degree of design flexibility with respect to previously reported ones. The key factor to these advantages is the dual shunt branch circuit of the proposed MTM TL, which significantly reduces the number of cells.

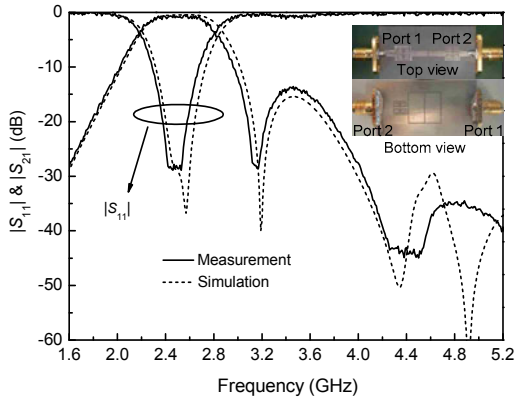

Fig. 7 Simulated and measured *S*-parameters of the fabricated BPF

4 Conclusions

A CRLH TL and its corresponding equivalent circuit model are studied. The CRLH TL features wide passband and an additional upper transmission zero. The cutoff frequencies have been well identified from theory, full-wave EM simulation, and circuit simulation. Novel CELC in the conductor strip has been exploited for the first time for the stopband performances which are attributing to the merged lower magnetic and upper electric resonances. Therefore, it is of practical interest in the design of controllable magnetic or electric resonators. By combining the CRLH TL with CELC, a BPF with good upper band skirt performance has been validated.

References

Amari, S., Rosenberg, U., 2004. Synthesis and design of novel in-line filters with one or two real transmission zeros. *IEEE Trans. Microw. Theory Tech.*, **52**(5):1464-1478. [doi:10.1109/TMTT.2004.827023]

Bonache, J., Gil, I., García-García, J., Martín, F., 2006. Novel microstrip bandpass filters based on complementary split-ring resonators. *IEEE Trans. Microw. Theory Tech.*, **54**(1):265-271. [doi:10.1109/TMTT.2005.861664]

Caloz, C., Itoh, T., 2006. Electromagnetic Metamaterials: Transmission Line Theory and Microwave Applications. John Wiley & Sons, Hoboken, New Jersey, CA.

Chen, W.L., Wang, G.M., 2009. Effective design of novel compact fractal-shaped microstrip coupled-line bandpass filters for suppression of the second harmonic. *IEEE Microw. Wirel. Compon. Lett.*, **19**(2):74-76. [doi:10.1109/LMWC.2008.2011311]

Falcone, F., Lopetegi, T., Laso, M.A.G., Baena, J.D., Bonache, J., Beruete, M., Marqués, R., Martin, F., Sorolla, M., 2004. Babinet principle applied to the design of metasurfaces and metamaterials. *Phys. Rev. Lett.*, **93**:197401. [doi:10.1103/PhysRevLett.93.197401]

García-García, J., Martín, F., Falcone, F., Bonache, J., Baena, J.D., Gil, I., Amat, E., Lopetegi, T., Laso, M.A.G., Iturmendi, J.A.M., *et al*., 2005. Microwave filters with improved stopband based on sub-wavelength resonators. *IEEE Trans. Microw. Theory Tech.*, **53**(6):1997-2006. [doi:10.1109/TMTT.2005.848828]

Hand, T.H., Gollub, J., Sajuyigbe, S., Smith, D.R., Cummer, S.A., 2008. Characterization of complementary electric field coupled resonant surfaces. *Appl. Phys. Lett.*, **93**:212504. [doi:10.1063/1.3037215]

Kim, I.K., Kingsley, N., Morton, M., Bairavasubramanian, R., Papapolymerou, J., Tentzeris, M.M., Yook, J.G., 2005. Fractal-shaped microstrip coupled-line bandpass filters for suppression of second harmonic. *IEEE Trans. Microw. Theory Tech.*, **53**(9):2943-2948. [doi:10.1109/TMTT.2005.854263]

Lu, M.Z., Chin, J.Y., Liu, R.P., Cui, T.J., 2008. A Microstrip Phase Shifter Using Complementary Metamaterials. Int. Conf. on Microwave and Millimeter Wave Technology, p.1569-1571. [doi:10.1109/ICMMT.2008.4540751]

Mandal, M.K., Mondal, P., Sanyal, S., Chakrabarty, A., 2006. Low insertion-loss, sharp rejection and compact microstrip low-pass filters. *IEEE Microw. Wirel. Compon. Lett.*, **16**(11):600-602. [doi:10.1109/LMWC.2006.884777]

Niu, J.X., 2010. Dual-band dual-mode patch antenna based on resonant-type metamaterial transmission line. *Electron. Lett.*, **46**(4):266-268. [doi:10.1049/el.2010.3142]

Schurig, D., Mock, J.J., Smith, D.R., 2006. Electric-field-coupled resonators for negative permittivity metamaterials. *Appl. Phys. Lett.*, **88**:041109. [doi:10.1063/1.2166681]

Tsai, C.M., Lee, S.Y., Lee, H.M., 2003. Transmission-line filters with capacitively loaded coupled lines. *IEEE Trans. Microw. Theory Tech.*, **51**(5):1517-1524. [doi:10.1109/TMTT.2003.810133]

Xu, H.X., Wang, G.M., Zhang, C.X., Wang, X., 2011a. Characterization of composite right/left-handed transmission line. *Electron. Lett.*, **47**(18):1030-1032. [doi:10.1049/el.2010.3707]

Xu, H.X., Wang, G.M., Zhang, C.X., Peng, Q., 2011b. Hilbert-shaped complementary single split ring resonator and low-pass filter with ultra-wide stopband, excellent selectivity and low insertion-loss. *Int. J. Electron. Commun.*, **65**(11):901-905. [doi:10.1016/j.aeue.2011.02.012]

Xu, H.X., Wang, G.M., Chen, P.L., Li, T.P., 2011c. Miniaturized fractal-shaped branch-line coupler for dual-band application based on composite right/left handed transmission lines. *J. Zhejiang Univ.-Sci. C (Comput. & Electron.)*, **12**(9):766-773. [doi:10.1631/jzus.C1000343]